the wavelength resolution is determined by the monochromator, whereas the timing and moderator characteristics determine the wavelength resolution on a time-of-flight instrument. Although the second term in equation (2.9.5.1) is standard in scattering, it has a unique characteristic, in that the angular divergence of the reflected beam determines the resolution. This is the case because the sample is a δ-function scatterer, so that the angle of the incident beam can be determined precisely by knowing the reflected angle (Hamilton, Hayter & Smith, 1994). For a more complete description of both types of neutron reflectometry instrumentation, see Russell (1990).

2.9.6. Resolution in real space

From Fig. 2.9.2.3, the period δQ of the reflectivity oscillation (in the region where the Born approximation becomes valid, sufficiently far away from the critical angle) is inversely proportional to the thickness t of the film. That is, $2\pi/(\delta Q) = t$. Consequently, in order to be able to resolve reflectivity oscillations for a film of thickness t, the instrumental Q resolution ΔQ [from equation (2.9.5.1)] must be approximately $2\pi/t$ or smaller. With sufficiently good instrumental resolution, even the thickness of a film with non-abrupt interfaces can be accurately determined, as demonstrated by the hypothetical case depicted in Fig. 2.9.6.1 (where the instrumental resolution is taken to be perfect): an overall film-thickness difference of 2 Å (between 42 and 40 Å films) is clearly resolved at a Q of about 0.2 Å^{-1}. In practice, differences even less than this can be distinguished. Note, however, that to 'see' more detailed features in the scattering-density profile (such as the oscillation on top of the plateau shown for the long-dash profile in the inset of Fig. 2.9.6.1), other than the overall film thickness, it can be necessary to make reflectivity measurements at values of Q corresponding to $2\pi/$(characteristic dimension of the feature).

2.9.7. Applications of neutron reflectometry

2.9.7.1. *Self-diffusion*

One of the simplest, yet powerful, examples of the use of neutron reflectivity is in the study of self-diffusion. Most techniques to measure diffusion coefficients rely on chemical and mechanical methods to measure density profiles after a sample

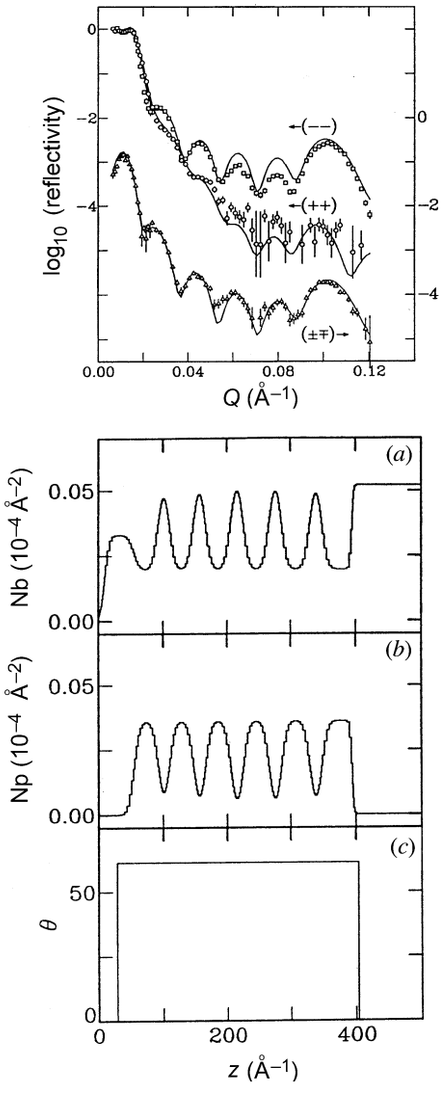

Fig. 2.9.7.3. Co/Cu(111) spin-dependent reflectivities (top). Nuclear (Nb) and magnetic (Np) scattering densities (bottom). Also shown is the (constant) moment direction [after Schreyer *et al.* (1993)].

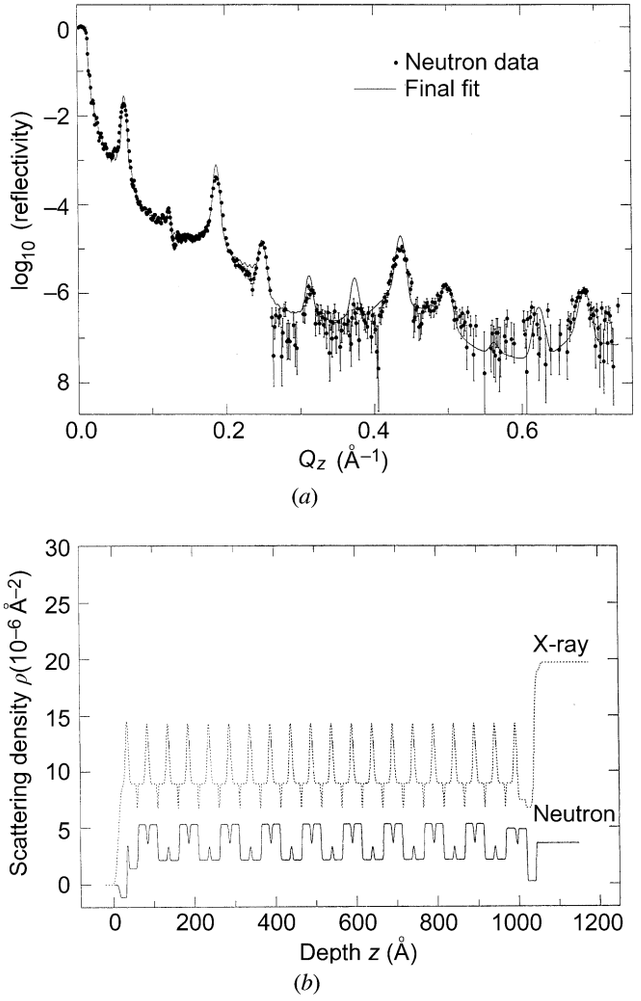

Fig. 2.9.7.4. (*a*) Measured neutron reflectivity for the Langmuir–Blodgett multilayer described in the text along with the fit. (*b*) Both corresponding neutron and X-ray scattering density profiles. The X-ray reflectivity is more sensitive to the high-Z barium in the head groups whereas the neutron reflectivity can distinguish mixing between adjacent hydrogenated and deuterated hydrocarbon tails [after Wiesler *et al.* (1995)].

has been annealed. Then a model for the diffusion is assumed, and the coefficients are calculated. Using standard techniques, researchers are unable to detect the movement of an atom through a sample of like atoms. However, using single bilayers of amorphous ^{10}B and ^{11}B, it was shown (Smith, Hamilton, Fitzsimmons, Baker, Hubbard, Nastasi, Hirvonen & Zocco, 1992) through neutron-reflectivity measurements that the diffusion of boron in boron could be measured by studying the density profile (see Figs. 2.9.7.1 and 2.9.7.2) of one isotope in the other as a function of annealing time. Also, because of the sensitivity of the technique to the interfacial density profile, it was found that standard Fickian diffusion models could not explain the measured density profiles.

2.9.7.2. *Magnetic multilayers*

In order to understand interlayer coupling mechanisms, it is necessary to know what the magnetic superstructure is for a given nonmagnetic spacer layer thickness and/or applied field strength. Fig. 2.9.7.3 shows the spin-dependent reflectivities for a Co/Cu (111) multilayer along with the nuclear (Nb) and magnetic (Np) scattering-density profiles deduced from the data of Schreyer, Zeidler, Morawe, Metoki, Zabel, Ankner & Majkrzak (1993). In this specific case, the in-plane ferromagnetic Co layers are themselves coupled ferromagnetically across the nonmagnetic Cu, all at a constant angle.

2.9.7.3. *Hydrogenous materials*

There are a substantial number of applications of neutron reflectometry in the study of hydrogenous films and multilayers, including diblock copolymer, surfactant, Langmuir–Blodgett, self-assembled monolayer, and lipid bilayer films. Reviews of the extensive research that has already been done have been written by Russell (1990) and Penfold & Thomas (1990). Only one specific example will be given here.

Fig. 2.9.7.4 shows neutron reflectivity data and the corresponding density profile for a Langmuir–Blodgett film composed of alternating bilayers of deuterated and hydrogenated stearic acid [after Wiesler, Feigin, Majkrzak, Ankner, Berzina & Troitsky (1995)]. Also shown in Fig. 2.9.7.4 is the scattering-density profile for the same sample as seen by X-rays. It is obvious that the X-rays are more sensitive to the high-Z barium in the head group, whereas the neutrons are especially good at distinguishing the degree of mixing between adjacent hydrogenated and deuterated hydrocarbon tails. This is a good example of the complementary nature of neutron and X-ray reflectivities.

References

2.1–2.2

Amorós, J. L., Buerger, M. J. & Amorós, M. C. (1975). *The Laue method*. New York: Academic Press.

Andrews, S. J., Hails, J. E., Harding, M. M. & Cruickshank, D. W. J. (1987). *Acta Cryst.* A**43**, 70–73.

Arndt, U. W. (1986). *X-ray position-sensitive detectors*. *J. Appl. Cryst.* **19**, 145–163.

Arndt, U. W. & Willis, B. T. M. (1966). *Single crystal diffractometry*. Cambridge University Press.

Arndt, U. W. & Wonacott, A. J. (1977). *The rotation method in crystallography*. Amsterdam: North-Holland.

Artymiuk, P. & Phillips, D. C. (1985). *On the design of diffractometers to measure a number of reflections simultaneously*. *Methods Enzymol.* **114**A, 397–415.

Bernal, J. D. (1927). *A universal X-ray photogoniometer*. *J. Sci. Instrum.* **4**, 273–284.

Bijvoet, J. M., Burgers, W. G. & Hägg, G. (1969). *Early papers on diffraction of X-rays by crystals*, Vol. I. Dordrecht: Kluwer Academic Publishers.

Bijvoet, J. M., Burgers, W. G. & Hägg, G. (1972). *Early papers on diffraction of X-rays by crystals*, Vol. II. Dordrecht: Kluwer Academic Publishers.

Blundell, T. L. & Johnson, L. N. (1976). *Protein crystallography*. New York: Academic Press.

Bonse, U., Materlik, G. & Schröder, W. (1976). *Perfect-crystal monochromators for synchrotron X-radiation*. *J. Appl. Cryst.* **9**, 223–230.

Bragg, W. H. (1928). *An introduction to crystal structure analysis*. London: Bell.

Bragg, W. L. (1949). *The crystalline state: a general survey*, pp. 30–33. London: Bell.

Brooks, I. & Moffat, K. (1991). *Laue diffraction from protein crystals using a sealed-tube X-ray source*. *J. Appl. Cryst.* **24**, 146–148.

Buerger, M. J. (1942). *X-ray crystallography*. New York: John Wiley.

Buerger, M. J. (1964). *The precession method*. New York: John Wiley.

Carr, P. D., Cruickshank, D. W. J. & Harding, M. M. (1992). *The determination of unit-cell parameters from Laue diffraction patterns using their gnomonic projections*. *J. Appl. Cryst.* **25**, 294–308.

Cassetta, A., Deacon, A., Emmerich, C., Habash, J., Helliwell, J. R., McSweeney, S., Snell, E., Thompson, A. W. & Weisgerber, S. (1993). *The emergence of the synchrotron Laue method for rapid data collection from protein crystals*. *Proc. R. Soc. London Ser. A*, **442**, 177–192.

Charpak, G., Demierre, C., Kahn, R., Santiard, J. C. & Sauli, F. (1977). *Some properties of spherical drift chambers*. *Nucl. Instrum. Methods*, **141**, 449.

Coppens, P. (1992). *Synchrotron radiation crystallography*. New York: Academic Press.

Cruickshank, D. W. J., Carr, P. D. & Harding, M. M. (1992). *Estimation of d_{min}, λ_{min} and λ_{max} from the gnomonic projections of Laue patterns*. *J. Appl. Cryst.* **25**, 285–293.

Cruickshank, D. W. J., Helliwell, J. R. & Moffat, K. (1987). *Multiplicity distribution of reflections in Laue diffraction*. *Acta Cryst.* A**43**, 656–674.

Cruickshank, D. W. J., Helliwell, J. R. & Moffat, K. (1991). *Angular distribution of reflections in Laue diffraction*. *Acta Cryst.* A**47**, 352–373.

Evans, H. T. & Lonsdale, K. (1959). *Diffraction geometry*. *International tables for X-ray crystallography*, Vol. II, p. 164. Birmingham: Kynoch Press.

Friedrich, W., Knipping, P. & von Laue, M. (1912). *Interferenz-Erscheinungen bei Röntgenstrahlen*. *Sitzungsber K. Bayer. Akad. Wiss. Muenchen*, pp. 303–322.

Glusker, J. P. & Trueblood, K. N. (1971). *Crystal structure analysis*, pp. 35–47. Oxford University Press.

Glusker, J. P. & Trueblood, K. N. (1985). *Crystal structure analysis*, 2nd ed., pp. 42–60. Oxford University Press.